

Nuclear Magnetic Resonance in Dilute Tin-Based Alloys

M. Daugherty and R. R. Hewitt

Department of Physics, University of California, Riverside, California 92502

(Received 24 September 1971)

The magnetic resonance of the ^{119}Sn nucleus has been observed in powdered samples of the tin-based alloys SnIn and SnSb at 4.2°K. The observed resonance line shapes cannot be explained without invoking the eddy-current mixing of the nuclear absorption and dispersion described by Chapman, Rhodes, and Seymour. A technique for analyzing the inhomogeneously broadened tin line shape is developed which takes this effect into account explicitly. This analysis is used to determine the concentration and field dependence of the isotropic and anisotropic Knight shifts, the unmixed single-crystal linewidth, and the eddy-current-mixing ratio for both alloy series. The isotropic Knight shift is found to be approximately independent of solute concentration to 2.0-at. % solute with $|(1/K)(dK/dc)| \leq 0.25$. The anisotropic Knight shift is linear in solute concentration with $(1/K_A)(dK_A/dc)$ being $+4.8 \pm 2.8$ in the SnIn alloys and -7.7 ± 0.5 in the SnSb alloys. The concentration and field dependence of the linewidth are in qualitative agreement with the scattering theory, and the concentration and field dependence of the eddy-current-mixing ratio are in good agreement with the theory of Chapman *et al.* The anomalous concentration dependence of the Knight shift in the dilute indium-rich alloys reported by Anderson, Thatcher, and Hewitt is shown to be the result of the concentration dependence of the eddy-current-mixing ratio in those alloys.

I. INTRODUCTION

Measurements recently reported by one of the authors^{1,2} have revealed the existence of an apparent anomaly in the concentration dependence of the ^{115}In isotropic Knight shift (K) in several series of indium-rich binary alloys. The anomalous feature observed was a sharp unexpected minimum in the concentration dependence of K between pure indium and 2.0-at. % solute. Since the scattering theory^{3,4} conventionally employed to explain solvent Knight shifts predicts that K is linear in solute concentration, the indium results have suggested⁵ the possibility of unexplained and previously undetected fine structure in the solvent Knight shifts in dilute binary alloys. In an effort to establish if similar anomalies exist in alloy systems based on solvents other than indium, we have conducted an experimental study of the ^{119}Sn NMR in the dilute tin-based alloys SnIn and SnSb between 0.0- and 2.0-at. % solute concentration.

Tin was chosen for this investigation because no systematic NMR measurements have previously been made in tin-based alloys and because tin is similar to indium in most of those aspects which were believed to offer possible explanations of the Knight-shift anomaly. The ^{119}Sn nucleus has a spin of $\frac{1}{2}$ and therefore, unlike indium, it possesses no electric quadrupole moment. As a result, the NMR spectrum of tin⁶⁻⁸ is considerably less complex than that of indium⁹ and is, thereby, amenable to a more exact line-shape analysis.

In order to make an accurate determination of the solute-concentration dependences of the K , the anisotropic Knight shift K_A , and the half-width at

half-maximum W of the single-crystal broadening, we have employed a new line-shape analysis for powdered tin. This analysis reveals that the observed line shapes are the result of eddy-current mixing of the absorptive and dispersive components of the nuclear susceptibility as described by Chapman, Rhodes, and Seymour.¹⁰ This mixing is characterized quantitatively by the eddy-current-mixing ratio β , which is defined as the ratio of the dispersive to the absorptive contributions to the line shape. By taking this effect into account explicitly in the line-shape analysis, we have been able to determine the solute-concentration dependence of β as well as the concentration dependences of K , K_A , and W . Using this analysis, we find no anomaly of the sort observed in the indium alloys in the concentration dependence of the ^{119}Sn isotropic Knight shift. However, we do find a maximum in the eddy-current-mixing ratio β at about 0.2-at. % solute concentration which appears to be, in part, the result of the transition from the normal-skin-effect regime, which obtains in the higher solute concentrations, to the anomalous-skin-effect regime obtaining in pure tin at 4.2°K. Proceeding from the results of the line-shape analysis, we have found that the existence of a similar maximum in the concentration dependence of β in the indium-based alloys is sufficient to explain the apparent anomaly observed in the isotropic Knight shifts in those alloys.

We begin in Sec. II with a description of the experimental procedure, and the line-shape analysis technique is described in Sec. III. The results obtained from this analysis are summarized and discussed in Sec. IV, and the conclusions are pre-

sented in Sec. V.

II. EXPERIMENTAL PROCEDURE

The $SnIn$ and $SnSb$ samples used were obtained in the form of 325-mesh powders from the Indium Corporation of America and were prepared from 99.999%-pure metals. Each of these alloy series comprised ten samples spanning the solute-concentration range from pure tin to 2.0-at.% solute in intervals of 0.2 at.%. The particle-size distribution of the samples was determined by using a microscope with an oil-immersion objective and a calibrated eyepiece to survey the particles in a typical sample.

All of the measurements were made at 4.2 °K and constant magnetic field (1.25, 5.5 and 10.0 kOe) using a frequency-swept marginal oscillator of the Pound-Knight-Watkins type.¹¹ The magnetic field was modulated at a frequency of 94 Hz with a peak-to-peak amplitude which did not exceed $\frac{1}{3}$ of the single-crystal linewidth, and the output of the marginal oscillator was phase-sensitive detected and recorded on an X-Y recorder. The frequency was measured to the nearest 10 Hz and recorded at regular intervals throughout the frequency sweep.

Because the primary objective of the experiment was to study the solute-concentration dependence of the ^{119}Sn resonance, one of the samples ($Sn_{0.999}In_{0.001}$) was chosen as a reference and run at the beginning and end of each series of measurements. The pure-tin sample was not used as a reference because of the large magnetoresistive pickup it produced and because the signal-to-noise ratio was better in the alloy samples. The value of the magnetic field during each series of measurements was determined by observing the ^{63}Cu resonance in a sample of pure-copper powder. The ^{119}Sn resonance was measured a minimum of twice in each alloy sample, once with the frequency increasing and once with it decreasing, so that the effects of the lock-in time constant could be averaged out. The reference sample was run more than 25 times at each field.

III. LINE-SHAPE ANALYSIS

The power absorbed by the ^{119}Sn nuclei in a crystallite of pure tin is described by the line-shape function $f(\nu)$, which is proportional to the absorptive component $\chi''(\nu)$ of the complex nuclear susceptibility:

$$f(\nu) \propto \chi''(\nu) = -\text{Im}[\chi(\nu)].$$

Since tin displays an axially symmetric anisotropic Knight shift, the function $f(\nu)$ is centered on the frequency ν_c given by

$$\nu_c = [1 + K + \frac{1}{3}K_A(3 \cos^2\theta - 1)]\nu_r, \quad (1)$$

where K and K_A are, respectively, the isotropic and anisotropic parts¹² of the Knight shift, ν_r is the resonance frequency of the ^{119}Sn nuclei in a non-conducting reference compound, and θ is the angle between the tetragonal symmetry axis [001] of the crystallite and the direction of the external magnetic field. NMR measurements on pure tin^{6,8,13} have indicated that, at liquid-helium temperatures, $f(\nu)$ is intermediate in shape between a Lorentzian and a Gaussian and that the experimental linewidth (i. e., the peak-to-peak linewidth of the derivative) depends on the orientation of the crystal in the magnetic field and averages over random orientations to between 1.0 and 1.5 kHz.

According to the scattering theory of Blandin and Daniel,³ the addition of random substitutional impurities into the tin lattice will set up Friedel oscillations in the electron charge density around the solute-impurity sites. These oscillations give rise to variations in the values of K and K_A at the solvent nuclei which in turn cause a variation in the value of ν_c given by (1). If we represent this distribution by the function $g_c(\nu_c)$, then the nuclear-absorption line-shape function $f_c(\nu)$ for a crystallite of tin alloy of solute concentration c will be given by the convolution

$$f_c(\nu) = \int_{-\infty}^{+\infty} f(\nu - \nu_c) g_c(\nu_c) d\nu_c. \quad (2)$$

The function $g_c(\nu_c)$ depends on the solute concentration c and is centered on the frequency $\bar{\nu}_c$ given by

$$\bar{\nu}_c(c) = \{1 + \bar{K}(c) + \frac{1}{3}[\bar{K}_A(c)](3 \cos^2\theta - 1)\}\nu_r, \quad (3)$$

where \bar{K} and \bar{K}_A are the mean values of K and K_A at the solvent nuclei. It is the solute-concentration dependences of \bar{K} , \bar{K}_A , and the half-width at half-maximum W of $f_c(\nu)$ which we wish to determine. The distribution function $g_c(\nu_c)$ is expected³ to be Lorentzian at low solute concentrations and to become more Gaussian in character at higher concentration. Thus for the solute concentrations employed in this study, we expect the line-shape function $f_c(\nu)$ to be proportional to the convolution (2) of the Lorentzian $g_c(\nu_c)$ with a symmetric curve $f(\nu)$ intermediate in shape between a Lorentzian and a Gaussian. Actually, the function $g_c(\nu_c)$, and, therefore, $f_c(\nu)$, need not be rigorously symmetric with respect to $\bar{\nu}_c$, although a calculation of $g_c(\nu_c)$ for indium² indicates that the asymmetry is probably small. This treatment also assumes that the function $f(\nu)$ appearing under the integral in (2) is independent of the crystal orientation angle θ , the solute concentration c or, for a fixed θ , the value of ν_c appropriate to a given packet of isochronous ^{119}Sn nuclei. The single-crystal measurements referred to above^{6,8} indicate that the pure-tin linewidth is a function of both the angle θ between the magnetic field and the [001] axis and the angle ϕ between the

[100] axis and the projection of the magnetic field onto the basal plane. Since the value of $\bar{\nu}_c$ appropriate to a given crystallite depends only on θ , the θ dependence of $f(\nu)$ can only be included in this analysis if the θ dependence of the average over ϕ of the width of $f(\nu)$ is known. Since neither this information nor the concentration dependence of $f(\nu)$ is available, the characterization of $f_c(\nu)$ as a symmetric shape given by (2) and centered on the frequency $\bar{\nu}_c$ is the best available approximation.

Chapman, Rhodes, and Seymour¹⁰ have shown that, if the characteristic dimensions of the sample are comparable to or larger than the skin depth, the power absorbed by the sample, and hence the observed line shape, will be proportional to a linear combination of the absorptive χ'' and dispersive χ' components of the nuclear susceptibility. For spherical particles, the value of the ratio β of the dispersive to the absorptive contributions is a function of the ratio p of the particle diameter d to the skin depth δ and is given in Fig. 4 of Ref. 10. For an alloy sample, the absorptive component of the nuclear susceptibility will be proportional to the convolution (2). Thus, by using one of the Kramers-Kronig relations to express the dispersive component in terms of the absorptive component, we can write the eddy-current-mixed line-shape function $f_{cm}(\nu)$ for an alloy as

$$f_{cm}(\nu) = f_c(\nu) + \frac{\beta}{\pi} \wp \int_{-\infty}^{+\infty} \frac{f_c(\nu')}{\nu' - \nu} d\nu'. \quad (4)$$

For powdered samples there is a distribution of values of θ for particles in the powder. The probability of any given angle θ will be proportional to $\sin\theta$, since it is proportional to the area subtended on the unit sphere by vectors with orientation angles between θ and $\theta + d\theta$. Thus, the powder line-shape function $F(\nu)$ is given by the integral

$$F(\nu) = \int_0^\pi f_{cm}(\nu) \sin\theta d\theta = \int_0^1 f_{cm}(\nu) d\mu, \quad (5)$$

where $\mu \equiv \cos\theta$ and $f_{cm}(\nu)$ depends on θ through the dependence of $f_c(\nu)$ on $\bar{\nu}_c$. The function $F(\nu)$, for $f(\nu)$ given by a δ function and for an eddy-current-mixing ratio of zero, is shown in Fig. 1(a). This function represents the distribution of frequencies $\bar{\nu}_c$ for crystallites in the powder. For $f(\nu)$ given by a symmetric curve of nonzero width and for β between 0 and 1, the function $F(\nu)$ is of the general form shown in Fig. 1(b). When phase-sensitive detection is employed, the observed signal $S(\nu)$ is the first derivative of $F(\nu)$, shown in Fig. 1(c). Therefore, the experimental line-shape function $S(\nu)$ is given by combining (4) and (5) and differentiating:

$$S(\nu) = \frac{d}{d\nu} \left[\int_0^1 \left(f_c(\nu) + \frac{\beta}{\pi} \wp \int_{-\infty}^{+\infty} \frac{f_c(\nu')}{\nu' - \nu} d\nu' \right) d\mu \right], \quad (6)$$

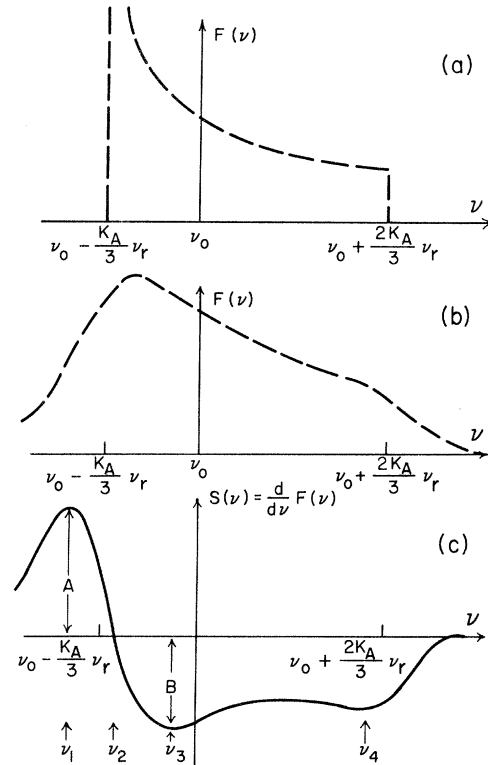


FIG. 1. (a) Powder-pattern line-shape function $F(\nu)$ for the single-crystal line-shape function $f(\nu)$ given by a δ function. The frequency ν_0 is defined as $(1+K)\nu_R$. (b) Typical form of $F(\nu)$ for $f(\nu)$ given by a symmetric curve and for β between 0 and 1. (c) Observed line-shape function $S(\nu)$, the first derivative of $F(\nu)$.

where $f_c(\nu)$ is given by the convolution (2). Since, for variations in frequency on the order of the linewidth, β is independent of ν , and since, for spherical particles, β is also independent of μ , (6) can always be written in the form

$$S(\nu) = S_a(\nu) + \beta S_d(\nu),$$

where $S_a(\nu)$ and $S_d(\nu)$ are, respectively, the absorptive and dispersive contributions to the observed line shape.

If $f_c(\nu)$ is given by a Lorentzian with half-width at half-maximum W , we find

$$f_c^L(\nu) = \frac{W}{2\pi^2} \frac{1}{W^2 + (\nu - \bar{\nu}_c)^2},$$

and then $S(\nu)$ is defined as $S^L(\nu) = S_a^L(\nu) + \beta S_d^L(\nu)$. $S_a^L(\nu)$ is given by Searle, Smith, and Wyard¹⁴ and will not be reproduced here, and $S_d^L(\nu)$ can be shown to be given by

$$S_d^L(\nu) = \frac{1}{2\pi^2} \int_0^1 \frac{(\bar{\nu}_c - \nu)^2 - W^2}{(\bar{\nu}_c - \nu)^2 + W^2} d\mu. \quad (7)$$

Suppose, on the other hand, $f_c(\nu)$ is given by a Gaussian

of half-width at half-maximum W

$$F_c^G(\nu) = \frac{1}{D(2\pi)^{3/2}} \exp\left(-\frac{(\nu - \bar{\nu}_c)^2}{2D^2}\right),$$

where

$$D = W/1.18.$$

Then $S(\nu)$ is defined as $S^G(\nu) = S_a^G(\nu) + \beta S_d^G(\nu)$, where

$$S_a^G(\nu) = \frac{-1}{D^3(2\pi)^{3/2}} \int_0^1 (\nu - \bar{\nu}_c) \exp\left(-\frac{(\nu - \bar{\nu}_c)^2}{2D^2}\right) d\mu, \quad (8)$$

$$S_d^G(\nu) = \frac{1}{\pi D^2} \int_0^1 [G(a) - 0.5] d\mu, \quad (9)$$

and $G(a)$ is given by

$$G(a) = ae^{-a^2} \int_0^a e^{x^2} dx.$$

The quantity $G(a)/a$ is known as Dawson's integral and is a tabulated function.¹⁵

The values of \bar{K} , \bar{K}_A , W , and β appropriate to a given powdered sample of tin alloy were determined by an iterative comparison of the experimentally observed line-shape function with the computer-generated function $S(\nu)$. This comparison was made for $f_c(\nu)$ given by both a Lorentzian and a Gaussian. Because of the large number of other parameters involved, no attempt was made to represent $f_c(\nu)$ by a shape intermediate between these two forms, even though the convolution (2) can be expected to be strictly Lorentzian (Gaussian) only if both $f(\nu)$ and $g_c(\nu_c)$ are Lorentzian (Gaussian). The functions $S^L(\nu)$ and $S^G(\nu)$ were generated by using Eqs. (3) and (6) and numerically evaluating the integrals in (7)–(9) as well as the function $S_a^L(\nu)$ given by Searle *et al.*

To make a comparison with the theoretical line shape, the experimental line was characterized by the four line-shape parameters R , $(\Delta\nu)_1$, $(\Delta\nu)_2$, and ν_Z , given by

$$R = A/B, \quad (\Delta\nu)_1 = \nu_3 - \nu_1,$$

$$(\Delta\nu)_2 = \nu_4 - \nu_1, \quad \nu_Z = \nu_2,$$

where A , B , and $\nu_1 - \nu_4$ are defined in terms of the line shape in Fig. 1(c). Initial guesses of the values of \bar{K} , \bar{K}_A , W , and β were first used to generate a trial function $S(\nu)$. The values of R , $(\Delta\nu)_1$, $(\Delta\nu)_2$, and ν_Z corresponding to this function were determined, and the differences between these values and the corresponding experimental values were used to make new guesses of the values of \bar{K} , \bar{K}_A , W , and β . This process was iterated until the differences between the experimental and computer-generated values of the line-shape parameters were all less than the accuracy with which the experimental parameters could be determined from the line, typically about 100 Hz for frequency measure-

ments. R , $(\Delta\nu)_1$, $(\Delta\nu)_2$, and ν_Z are most sensitive to the values of β , W , \bar{K}_A , and \bar{K} , respectively, so that the iteration procedure can be made rapidly convergent. This procedure, referred to hereafter as the type-I data-reduction scheme, worked well except at high solute concentrations or low magnetic fields where the powder-pattern linewidth $K_A \nu_r$ became comparable to the width $2W$ of the symmetric broadening $f_c(\nu)$. Under these conditions, the peaks in $S(\nu)$ at ν_3 and ν_4 merged, and it was necessary to employ a second line-shape analysis (type II) in which $(\Delta\nu)_1$ and $(\Delta\nu)_2$ were redefined as the width of the peak at ν_1 and the ratio of the width of the peak at ν_3 to the width at ν_1 , respectively. This program converged less rapidly and was characterized by more scatter in the results than the type-I reduction scheme.

The typical effects of eddy-current mixing on the line-shape function are evident in Fig. 2, which shows $S(\nu)$ for $f_c(\nu)$ given by a Lorentzian of half-width 1.0 kHz and for values of β of 0 (dashed line) and 1 (solid line). Figure 2 indicates that an increase of the eddy-current-mixing ratio from 0 to 1 has two major impacts on the line shape; it reduces the asymmetry ratio R from a value near 3 to a value of about 1, and it shifts the position of the line downward in frequency by about 60% of the half-width W . It is important to note that, whereas the increase of β causes an increase in the asymmetry of the single-crystal NMR line shape, it has the opposite effect on the tin-powder line shape. Failure to recognize this distinction has led¹⁶ to the erroneous conclusion that the almost symmetric line shapes (e. g., $R = 1.4$) displayed by powdered-tin samples imply little or no eddy-current mixing.

IV. RESULTS AND DISCUSSION

The experimental data for the reference sample ($Sn_{0.999}In_{0.001}$) at 10 kOe and the corresponding iteratively fit line-shape functions for Lorentzian (solid line) and Gaussian (dashed line) broadening are shown in Fig. 3. The values of \bar{K} , \bar{K}_A , W , and

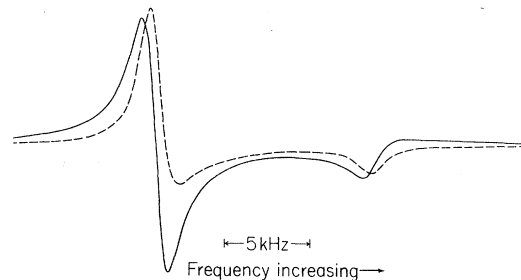


FIG. 2. Line-shape function $S(\nu)$ for $f(\nu)$ given by a Lorentzian of half-width 1.0 kHz and for values of the eddy-current-mixing ratio β of 0 (dashed line) and 1 (solid line).

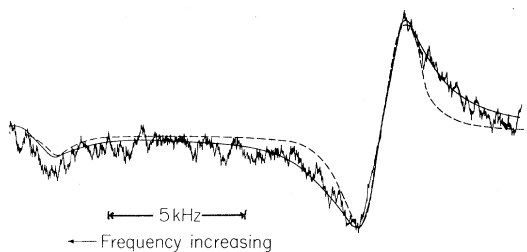


FIG. 3. Experimental data for the reference sample ($\text{Sn}_{0.999}\text{In}_{0.001}$) at 10 kOe and the corresponding iteratively fit line-shape functions for Lorentzian (solid line) and Gaussian (dashed line) broadening. The values obtained from the two fits are given in Table I.

β obtained for this line from the type-I data-reduction scheme are in Table I. These data display two features characteristic of all the results: first, that the eddy-current-mixing ratio is markedly nonzero, and second, that the observed line shapes are better fit by Lorentzian than Gaussian broadening. Lorentzian broadening was found to provide a somewhat better fit at all solute concentrations studied, although the disparity was most apparent in the low-concentration alloys. All of the results presented here correspond to the assumption of an angularly independent Lorentzian single-crystal line-shape function $f_c(\nu)$.

Representative results for \bar{K} , \bar{K}_A , W , and β are shown in Figs. 4–7. The open (closed) circles represent the results of the type-I (-II) data-reduction program, and the triangles represent the average of the two values when both programs were used. The error bars represent the standard deviation of the values obtained for the reference sample or the variation in the values obtained for the sample in question, whichever was the greater. The type-II points generally displayed considerably more scatter than the type-I points, and, because only the type-II program could be applied to the data taken at 1.25 kOe, the low-field results were not used.

A. Isotropic Knight Shift

The values of the isotropic Knight shift \bar{K} for the SnIn and SnSb alloys are presented in Fig. 4 in terms of the differences $\Delta\bar{K}$ between \bar{K} for a given alloy and \bar{K} for the reference sample. No anomaly of

TABLE I. Values of \bar{K} , \bar{K}_A , W , and β obtained for the reference-sample ($\text{Sn}_{0.999}\text{In}_{0.001}$) data shown in Fig. 3.

Line-shape parameter	\bar{K} (%)	\bar{K}_A (%)	W (kHz)	β
Lorentzian	0.705	0.080	1.10	0.80
Gaussian	0.710	0.080	0.80	0.25

the type reported for the indium alloys is observed. \bar{K} is approximately independent of concentration with $|\Delta\bar{K}/\bar{K}| \leq \frac{1}{2}\%$ or $(1/\bar{K})(d\bar{K}/dc) = 0.0 \pm 0.25$. Since we were primarily interested in the concentration dependence of \bar{K} , no attempt was made to make an accurate absolute determination of K for pure tin. However, relative to a value of $\gamma/2\pi$ of 15.870 MHz/(10 kG), the value of K in the pure-tin sample was found to be $(0.706 \pm 0.003)\%$ at 10 kOe and $(0.703 \pm 0.003)\%$ at 5.5 kOe.

The small slope of the isotropic Knight shift vs solute concentration is consistent with results in other polyvalent metals in which $(1/\bar{K})(d\bar{K}/dc)$ is smaller than predicted by the scattering theory.¹⁷ In the particular case of lead, the only other tetravalent solvent studied, Snodgrass and Bennett¹⁸ found values of $(1/\bar{K})(d\bar{K}/dc)$ which were only 8% of that predicted by theory. The solute-concentration range studied here was too narrow to allow accurate determination of such small values of $(1/\bar{K})(d\bar{K}/dc)$. For this reason and because the anisotropic band structure of tin¹⁹ is not well represented by the assumption of a nearly spherical Fermi surface, we have not compared our results with the scattering theory.

B. Anisotropic Knight Shift

The anisotropic Knight shift (Fig. 5) is found to be approximately linear in solute concentration, increasing in the SnIn alloys and decreasing in the SnSb alloys. The average of the values of $(1/\bar{K}_A) \times (d\bar{K}_A/dc)$ obtained at 10 and 5.5 kOe was 4.8 ± 2.8

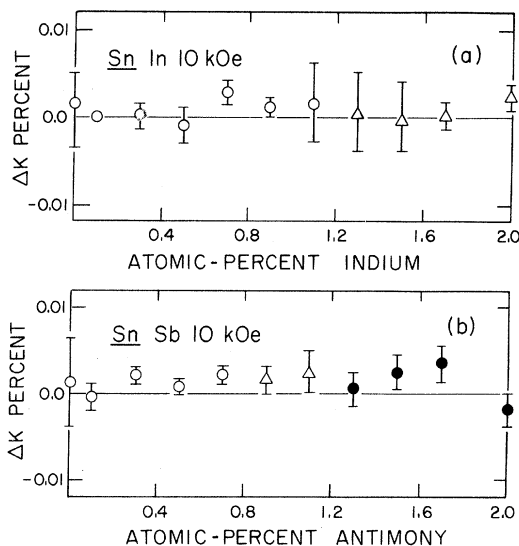


FIG. 4. Concentration dependence of the tin isotropic Knight shift relative to the reference sample ($\text{Sn}_{0.999}\text{In}_{0.001}$) in terms of the differences $\Delta\bar{K}$ between \bar{K} , for a given alloy and \bar{K} , for the reference sample. (a) SnIn and (b) SnSb alloys at 10 kOe.

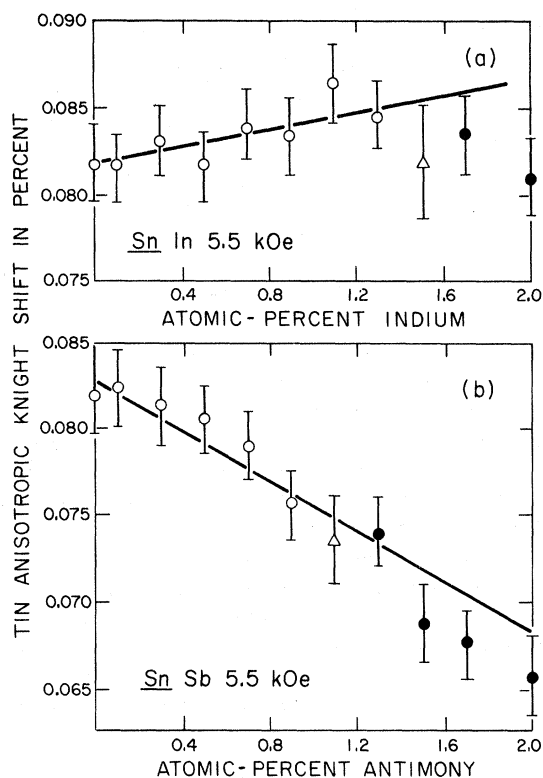


FIG. 5. Concentration dependence of the anisotropic Knight shift K_A in the (a) SnIn and (b) SnSb alloys at 5.5 kOe.

in the SnIn alloys and -7.7 ± 0.5 in the SnSb alloys, where the uncertainties represent the variation between the values obtained at the two fields. Since the type-II points were generally found to lie below the line which best fit the type-I points, they were not weighted equally in the determination of the slopes. The value of K_A in pure tin was found to be $(0.082 \pm 0.002)\%$ at both fields, in excellent agreement with previous measurements.^{6,7}

The solute-concentration dependence of the anisotropic Knight shift may reflect band-structure effects arising from the change in the number of conduction electrons which occurs with the addition of solutes of valence different from the host. For example, Lee and Raynor²⁰ have measured the concentration dependence of the lattice parameters a and c in SnIn and SnSb . They found that c remained essentially constant while a varied in opposite directions for the two solutes. The ratio of the slope of a vs the concentration for the SnSb alloys to the same slope in the SnIn alloys was -1.9 ± 0.2 . The same ratio for the slopes of K_A vs concentration, determined from this work, is -1.6 ± 1.2 . While the uncertainty in this number is sufficiently large that the agreement may be fortuitous, the relative signs and magnitudes suggest that the concentration dependence of the anisotropic Knight shift may well

be amenable to a rigid-band explanation similar to the one applied to the concentration dependence of the lattice parameters.

C. Linewidth

The half-width at half-maximum W of the unmixed single-crystal line-shape function (Fig. 6) was found to depend approximately parabolically on solute concentration and linearly on magnetic field.

The mean values of W obtained for pure tin were 0.7 ± 0.1 kHz at 5.5 kOe and 0.8 ± 0.1 kHz at 10 kOe.

The fact that the observed line shapes are better fit by Lorentzian than Gaussian broadening supports the argument of Sec. II that the unmixed single-crystal line-shape function $f_c(\nu)$ is given by convolution (2) of a Lorentzian with a symmetric curve intermediate between a Lorentzian and a Gaussian. The representation of $f_c(\nu)$ by a Lorentzian should be best at the low solute concentrations with the line becoming more Gaussian both in pure tin, for which $g_c(\nu_c)$ is a δ function, and in the higher-concentration alloys. Since the assumption that the symmetric broadening is independent of θ produces reasonably good agreement with the line shape, it seems likely that the θ dependence of the average over ϕ of the half-width at half-maximum of $f_c(\nu)$ is not strong. However, because the width $(\Delta\nu)_1$ of the broadened powder-pattern singularity at $\nu = (1 + K - \frac{1}{3}K_A)\nu_R$ (i. e., $\theta = \frac{1}{2}\pi$) was the line-shape parameter most strongly influenced by the choice

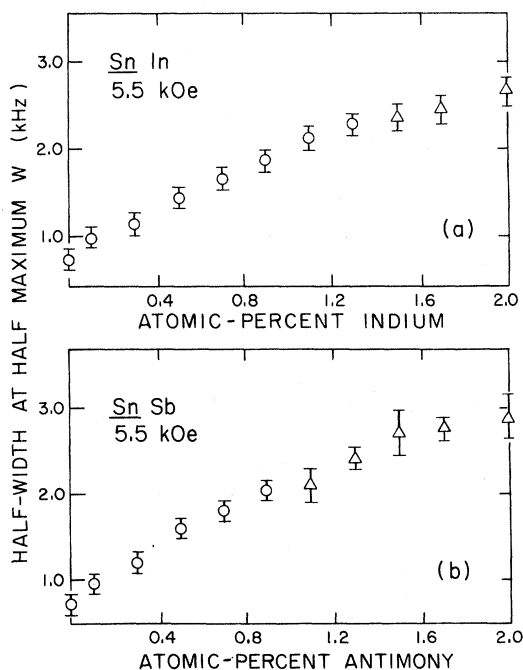


FIG. 6. Concentration dependence of the half-width at half-maximum W of the unmixed single-crystal line-shape function for the (a) SnIn and (b) SnSb alloys at 5.5 kOe.

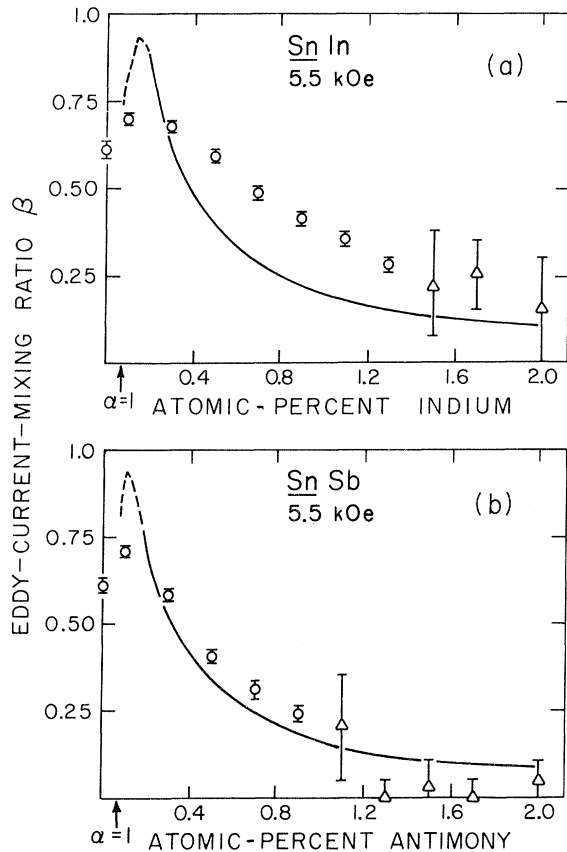


FIG. 7. Concentration dependence of the eddy-current-mixing ratio β for the (a) SnIn and (b) SnSb alloys at 5.5 kOe. The smooth curves represent the prediction of the normal-regime theory of Chapman *et al.* (Ref. 10). The dashed portion of the curve designates the region for which $0.6 \leq \alpha^{1/6} \leq 1.0$.

of W in the line-shape-analysis program, the values of W in Fig. 6 are best interpreted as the averages over ϕ of the half-width of $f(\nu)$ for $\theta = \frac{1}{2}\pi$. Sharma⁸ has measured the ϕ dependence of the pure-tin experimental linewidths for $\theta = \frac{1}{2}\pi$. His measurements indicate that the average over ϕ of the peak-to-peak width of the derivative is about 1.0 kHz. For a Lorentzian this corresponds to a mean half-width W of about 0.86 kHz compared to a value of about 0.75 kHz obtained from this experiment.

The concentration and field dependence of W can be compared with the scattering theory in the following way. If we make the self-consistent assumptions that $f_c(\nu)$, $f(\nu)$, and $g_c(\nu_c)$ are all Lorentzians, then the half-width W of $f_c(\nu)$ will be given by

$$W = W_f + W_g, \quad (10)$$

where W_f and W_g are the half-widths of $f(\nu)$ and $g_c(\nu_c)$, respectively. Rowland's⁴ derivation of the concentration and field dependence of the contribution to the second moment of the line arising from

the inhomogeneous isotropic Knight shift can be extended to include the anisotropic Knight shift so that the angular average of the second moment of $g_c(\nu_c)$ is given by

$$\langle \Delta\nu^2 \rangle \propto c(1-c)\nu_r^2, \quad (11)$$

where c is the solute concentration in atomic fraction. The second moment of a Lorentzian is infinite, so $g_c(\nu_c)$ must be taken to be a truncated Lorentzian for which the half-width at half-maximum W_g is proportional to the square root of the finite second moment. Using this proportionality and combining Eqs. (10) and (11) yields, for small solute concentrations,

$$(W - W_f)^2 / \nu_r^2 \propto c(1-c) \approx c.$$

The quantity $(W - W_f)^2 / \nu_r^2$ is plotted vs solute concentration for the SnIn alloys in Fig. 8. The triangles and closed circles represent the results from the 5.5- and 10-kOe data, respectively. Considering the approximations made and the fact that ν_r^2 varies by a factor of 3.5 between the two fields, the agreement between the slopes is relatively good. The slight positive curvature may originate in the changing character of the line shape with increasing solute concentrations. Application of the Gaussian-line-shape-analysis program generally resulted in smaller values of W than did the Lorentzian program, and thus the values of W in the higher concentrations may be somewhat too large.

D. Eddy-Current-Mixing Ratio

The concentration dependence of the eddy-current-mixing ratio β is displayed in Fig. 7. At all

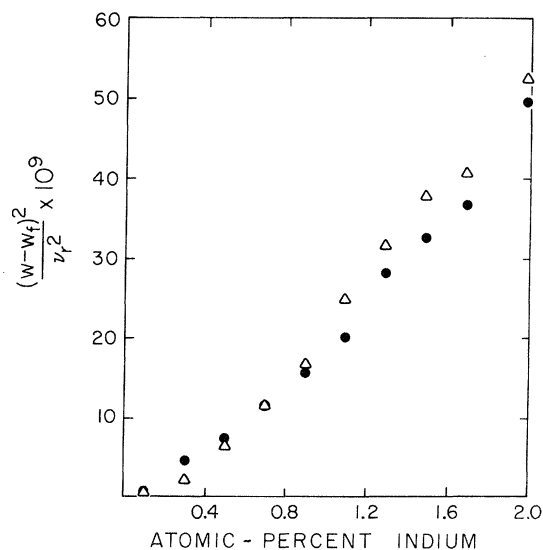


FIG. 8. Comparison of the width data with the predictions of the scattering theory for the SnIn alloys; triangle, 5.5-kOe results; closed circle, 10.0-kOe results.

three magnetic fields β was greatest in the low-concentration samples and decreased with increasing solute concentration, decreasing most rapidly in the low-field data. The maximum in β near 0.2 at. % in the 5.5-kOe results also appears in the SnIn results at 10 kOe but was not resolved in the SnSb results at that field.

The smooth curves in Fig. 7 represent the concentration dependence of β as predicted by the normal-regime eddy-current-mixing theory of Chapman *et al.*¹⁰ Their theoretical expression for small spherical particles was extended to the case of a powder of irregularly shaped particles by representing the powder as an assembly of identical spheres of diameter d equal to the mean equivalent diameter \bar{d} of the actual powdered sample. The equivalent diameter \bar{d} was determined by surveying the particles in a typical sample using an oil-immersion-objective microscope. Each particle was classified as either a sphere or a cylinder. Since the orientation of the cylinders in the rf magnetic field was random, they were taken to be equivalent to spheres of diameter d such that the average distance to the nearest surface for a point inside the particle was the same for the cylinder and its equivalent sphere. The mean diameter \bar{d} was then obtained by averaging the individual diameters weighted by the volume of the sphere within one skin depth of the surface. This weighting was used as an approximate means of taking account of the fact that most of the rf power absorbed by a powdered sample is absorbed by the larger particles. Since the skin depth is a function of the solute concentration, \bar{d} was concentration dependent, but, for concentrations above 0.1 at. %, this dependence was not rapid. The averaging procedure yielded a value of \bar{d} of about 22 μm for the 325-mesh samples surveyed. The theoretical values of β appropriate to each concentration were then obtained from the expression given by Chapman *et al.*¹⁰ by using the residual resistivities of the tin alloys measured by Burckbuchler and Reynolds²¹ to compute the classical skin depth δ and taking p to be \bar{d}/δ .

According to theory, as the solute concentration is decreased and p increases from 0, β goes from 0 through (i) a maximum of about 0.95 near $p = 4$, (ii) a minimum of about 0.65 near $p = 7$, and (iii) is slowly asymptotic to unity as p tends to infinity. For these alloys, at a frequency of 8.8 MHz (5.5 kOe) and 4.2 °K, the maximum in β should occur at about 0.2 at. % and, if the contribution of the surface scattering to the resistivity is neglected, the minimum will occur near 0.05 at. %. However, computation of the electron mean free path l , using the value of σ/l for tin determined by Reuter and Sondheimer,²² indicates that the sample will be in the anomalous-skin-effect regime [i. e., $\alpha^{1/6}$

$= (\frac{3}{2} l^2/\delta^2)^{1/6} > 1$] for solute concentrations below about 0.08 at. %. No theory of the eddy-current mixing for small particles in the anomalous regime is available. However, Allen and Seymour²³ have computed β for a semi-infinite flat plate in the anomalous regime as a function of $\alpha^{1/6}$. They find that as $\alpha^{1/6}$ is increased, β decreases from its normal-regime value of unity and is asymptotic to $1/\sqrt{3}$ as $\alpha^{1/6}$ goes to infinity. In experiments on foils of aluminum, they found that β began to diverge appreciably from its normal-regime value when $\alpha^{1/6}$ exceeded 0.6. For the tin alloys, this value corresponds to a solute concentration of about 0.2 at. %. Thus, if the behavior of β as a function of $\alpha^{1/6}$ for spherical particles is qualitatively similar to that for a flat plate, β should be below its normal-regime value for solute concentrations below about 0.2 at. %. This region is indicated by the dashed portion of the curve in Fig. 7. In view of the fact that the actual sample powders contained a distribution of particle sizes, and, therefore, a distribution of values of β for any given sample, it seems unlikely that the sharp maximum in the theoretical values of β between 0.1 and 0.2 at. % could be well resolved experimentally. The maximum observed in the concentration dependence of β is apparently the result of the superposition of the normal-regime maximum between 0.1 and 0.2 at. % and the decrease in β due to the onset of the anomalous regime at small solute concentrations. Regardless of the relative importance of these two effects in producing the observed maximum, the anomalous skin effect must be invoked to explain the fact that the value of β measured in the pure-tin sample is less than the value of β at the minimum in the normal-regime theory. It is interesting to note that, if the symmetric broadening is more Gaussian in pure tin than in the low-concentration alloys, the value of β in pure tin will be even lower since, for a given line shape, the Gaussian-data-reduction program was found to yield smaller values of β than the Lorentzian program.

E. Indium Experiment

We are now in a position to explain the results in the indium alloys.^{1,2} The indium Knight shifts were determined by measurements of the frequencies corresponding to three of the ten singularities in the powder pattern. However, because it is of the same form as the singularity at $(1 + K - \frac{1}{3} K_A)\nu_r$ in the tin powder pattern, we restrict our consideration to the frequency of the $\theta = \frac{1}{2}\pi$ singularity corresponding to the $|+\frac{1}{2}\rangle \leftrightarrow |-\frac{1}{2}\rangle$ transition in indium and designated as ν_1 . The results of the tin-line-shape analysis indicate that the downward frequency shift $\delta\nu$ in the zero crossing of the experimental line shape corresponding to

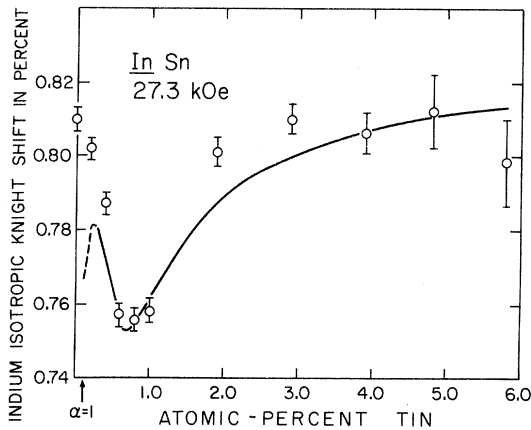


FIG. 9. Comparison of the indium-alloy Knight-shift data of Anderson *et al.* (Ref. 1) with the predictions of the eddy-current-mixing theory. The dashed portion of the curve designates the region for which $0.6 \leq \alpha^{1/6} \leq 1.0$.

this type of singularity is given by

$$\delta\nu \approx 0.6\beta W,$$

where W is the half-width of the unmixed symmetric broadening and β is the eddy-current-mixing ratio. If we extend this result to the shift $\delta\nu_i$ of the apparent center of the ^{115}In line at ν_i , the change $\delta\bar{K}$ in the apparent Knight shift will be given by

$$\delta\bar{K} = \frac{\delta\nu_i}{\nu_r} \approx \frac{0.6\beta W}{2.54 \times 10^7}, \quad (12)$$

where the value of ν_r used here is appropriate to the magnetic field of 27.3 kOe used in the indium measurements. Since they exhibit the most clearly defined minimum, we consider the specific case of the InSn alloys. The change $\delta\bar{K}$ for these alloys was computed from Eq. (12) by using the residual resistivities quoted by Thatcher²⁴ to compute β and the values of W measured by Anderson *et al.*¹ The results of this computation are compared with the experimental results in Fig. 9. The position of the smooth curve representing $\delta\bar{K}$ has been adjusted vertically to agree with the measured Knight shift at 4.0-at.-% Sn. The minimum in \bar{K} at about 0.8-at.-% Sn corresponds to the maximum in the normal-regime value of β at $p=4$. This maximum occurs at a higher concentration and is better resolved in the indium alloys than in the tin alloys because the residual resistivities of the indium alloys are lower and the frequency employed was higher. The decline of $\delta\bar{K}$ for pure indium to a value near 0 is apparently due to the decrease of β with the onset of the anomalous skin effect since $\alpha^{1/6} > 0.6$ for concentrations below about 0.25-at.-% Sn. The excellent agreement which this explanation provides with the position and magnitude of

the minimum in \bar{K} makes it clear that the observed anomaly is an artifact of the concentration dependence of the eddy-current-mixing ratio rather than the result of a concentration dependence of the electronic susceptibility in indium. This conclusion is consistent with the recent work of McLaughlin, Williamson, and Butterworth,²⁵ which shows no extremum in the concentration dependence of T_1T in the indium alloys.

V. CONCLUSION

The results of this study are in good agreement with the qualitative predictions of the scattering theory for the concentration and field dependence of the Knight shifts and linewidths as well as with the predictions of the normal-regime theory of Chapman *et al.*¹⁰ for the concentration and field dependence of the eddy-current-mixing ratios. However, the results also indicate that the behavior of the eddy-current-mixing ratio for small particles in the anomalous-skin-effect regime is not well understood.

The effects of eddy-current mixing on the NMR spectrum of indium were neglected by Anderson, Thatcher, and Hewitt¹ on the basis of the fact that the pure-indium Knight shift was found to be the same in the 325-mesh sample as in a sample consisting of 2- μm particles. Likewise, Karimov and Shchegolev¹⁶ cited similar results in powdered-tin samples as evidence that the eddy-current-mixing ratio was less than predicted by theory. However, an analysis of their line shape yields a value of β of about 0.6, in agreement with the results of this work. These facts suggest that, in the anomalous-skin-effect regime, β may be relatively insensitive to particle size and that the particle-size dependence of the position or shape of the NMR line does not therefore always constitute a useful test of the magnitude of the eddy-current mixing.

In the absence of a more complete anomalous-regime theory, reliable results from NMR measurements on powdered samples of pure metals or dilute alloys at low temperatures can only be achieved through the use of a crossed-coil NMR spectrometer in which the dispersive contribution can be balanced out or by the application of a line-shape analysis which determines the value of β self-consistently with the other variables which determine the shape and position of the line. Failure to take eddy-current mixing into account explicitly can lead to spurious temperature, field, and solute-concentration dependences in the measured Knight shifts and linewidths.

ACKNOWLEDGMENTS

The authors would like to acknowledge the insight provided by numerous discussions with D. E. MacLaughlin and F. C. Thatcher.

- ¹W. T. Anderson, F. C. Thatcher, and R. R. Hewitt, *Phys. Rev.* **171**, 541 (1968).
- ²F. C. Thatcher and R. R. Hewitt, *Phys. Rev. B* **1**, 454 (1970).
- ³A. Blandin and E. Daniel, *J. Phys. Chem. Solids* **10**, 126 (1959).
- ⁴T. J. Rowland, *Phys. Rev.* **125**, 459 (1962).
- ⁵R. E. Watson, L. H. Bennett, and A. J. Freeman, *Phys. Rev.* **179**, 590 (1969).
- ⁶E. P. Jones and D. L. Williams, *Can. J. Phys.* **42**, 1499 (1964).
- ⁷F. Borsa and R. G. Barnes, *J. Phys. Chem. Solids* **25**, 1305 (1964).
- ⁸S. N. Sharma, thesis (University of British Columbia, 1967) (unpublished).
- ⁹J. F. Adams, B. F. Williams, and R. R. Hewitt, *Phys. Rev.* **151**, 238 (1966).
- ¹⁰A. C. Chapman, P. Rhodes, and E. F. W. Seymour, *Proc. Phys. Soc. (London)* **B70**, 345 (1957).
- ¹¹R. V. Pound and W. D. Knight, *Rev. Sci. Instr.* **21**, 219 (1950).
- ¹²The anisotropic Knight shift is often defined as $\frac{2}{3}$ of this quantity, in which case $\nu_c = [1 + K + \frac{1}{2}K_A(3 \cos^2\theta - 1)]\nu_n$.
- ¹³H. Alloul and R. Deltour, *Phys. Rev.* **183**, 414 (1969).
- ¹⁴J. W. Searle, R. C. Smith, and S. J. Wyard, *Proc. Phys. Soc. (London)* **A74**, 491 (1959).
- ¹⁵M. Abramowitz and I. Stegun, *Handbook of Mathematical Functions* (U. S. GPO, Washington, D. C., 1964), Natl. Bur. Std. (U. S. Math.) Ser. 54, p. 319.
- ¹⁶Yu. S. Karimov and I. F. Shchegolev, *Zh. Eksperim. i Teor. Fiz.* **40**, 1289 (1960) [*Sov. Phys. JETP* **13**, 908 (1961)].
- ¹⁷D. A. Rigney and C. P. Flynn, *Phil. Mag.* **15**, 1213 (1967).
- ¹⁸R. J. Snodgrass and L. H. Bennett, *Phys. Rev.* **134**, A1295 (1964).
- ¹⁹G. Weisz, *Phys. Rev.* **149**, 504 (1966).
- ²⁰J. A. Lee and G. V. Raynor, *Proc. Phys. Soc. (London)* **B67**, 737 (1954).
- ²¹F. V. Burckbuchler and C. A. Reynolds, *Phys. Rev.* **175**, 550 (1968).
- ²²G. E. H. Reuter and E. H. Sondheimer, *Proc. Roy. Soc. (London)* **A195**, 336 (1948).
- ²³P. S. Allen and E. F. W. Seymour, *Proc. Phys. Soc. (London)* **82**, 174 (1963).
- ²⁴F. C. Thatcher, Ph.D. dissertation (University of California, Riverside, 1969) (unpublished).
- ²⁵D. E. MacLaughlin, J. D. Williamson, and J. Butterworth, *Phys. Rev. B* **4**, 60 (1971).

Magic-Angle NMR Experiments in Solids*

M. Mehring[†] and J. S. Waugh

*Department of Chemistry and Research Laboratory of Electronics,
Massachusetts Institute of Technology, Cambridge, Massachusetts 02139*

(Received 1 September 1971)

The time dependence of different interaction Hamiltonians of nuclear spins as encountered in NMR experiments where the external field is applied at the "magic angle" in the rotating frame is treated with the average Hamiltonian theory. First- and second-order correction terms of the average Hamiltonian are obtained for symmetric and antisymmetric cycles. New types of pulsed "magic-angle" experiments are treated in detail and experiments are performed to show their capability to resolve chemical shifts in solids. It is shown that such magic-angle methods, employed with applied fields of high duty factor, in principle offer advantages in the high-resolution NMR of solids over resonant multiple-pulse schemes. The problem of observing the nuclear-precession signal during applications of the strong fields is solved by "nesting" an observing cycle of low duty factor into the continuous or quasicontinuous irradiation sequence.

I. INTRODUCTION

The magnetic dipolar Hamiltonian \mathcal{H}_D of nuclei with spin I can be expressed as a scalar product of two second-rank tensor operators¹⁻⁴ representing its spatial and spin symmetry, respectively. Experiments have been performed utilizing this symmetry in which one operates on one or the other tensor in order to cancel out the dipolar Hamiltonian.

The first class of experiments involves spinning the sample^{5,6} with the rotation axis tilted by an angle θ with respect to the magnetic field H_0 , whereas in the second class, irradiation with strong

rf fields produces an effective field H_{eff} , which is tilted by an angle β with respect to H_0 .⁷⁻¹⁰ In both cases the Hamiltonian becomes time dependent in a periodic fashion with a certain period or cycle time t_c . In case the cycle time is short enough to allow coherent averaging, the Hamiltonian of the system can be replaced by an average Hamiltonian,¹⁰ expressed as a sum of different correction terms:

$$\bar{\mathcal{H}} = \bar{\mathcal{H}}^{(0)} + \bar{\mathcal{H}}^{(1)} + \bar{\mathcal{H}}^{(2)} + \dots, \quad (1a)$$

where

$$\bar{\mathcal{H}}^{(0)} = t_c^{-1} \int_0^{t_c} dt \bar{\mathcal{H}}(t),$$